JCTC Journal of Chemical Theory and Computation

Article

pubs.acs.org/JCTC

Investigating Disjoint Non-Kekulé Diradicals with Quantum Monte Carlo: The Tetramethyleneethane Molecule through the Jastrow Antisymmetrized Geminal Power Wave Function

Matteo Barborini*,† and Emanuele Coccia*,‡

†S3 Research Center, CNR-NANO, Via Campi 213/a, 41125 Modena, Modena, Italy

‡Laboratoire de Chimie Théorique, Sorbonne Universités, UPMC Univ Paris 06 & CNRS, UMR 7616, F-75005 Paris, France

Supporting Information

ABSTRACT: Disjoint non-Kekulé molecules are diradicals that present two independent radical centers and can violate Hund's rule, according to which the ground state should have triplet spin symmetry. The prototype of this class of systems is the tetramethyleneethane (TME) molecule for which indeed ion photoelectron spectroscopy (IPS) experiments revealed the singlet ^1A state to be more stable than the triplet ^3B_u. In this work we investigate the potential energy curves of the two spin states of TME and of the two anionic states of TME^- (^2A and $^2B_1$) as a function of the torsion of the central dihedral angle, with quantum Monte Carlo methods and a Jastrow Antisymmetrized Geminal Power wave function. Through *ab initio* geometrical optimizations we study the possible structural interconversions between the states, finding results which are in full agreement with the IPS experimental data.

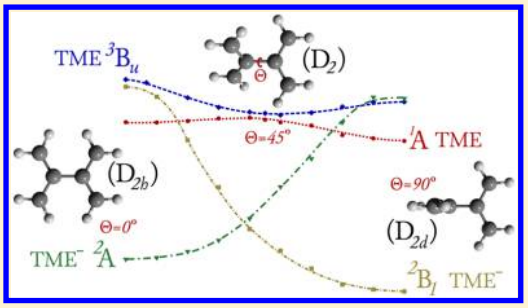

INTRODUCTION

Non-Kekulé molecules are fully conjugated moieties that cannot be represented by canonical Kekulé structures but contain at least two non-π-bonded atoms[1−3] responsible for a diradical or multiradical character. Diradicals are systems where two unpaired electrons occupy two (nearly)-degenerate molecular orbitals.[4,5] The spin−spin interactions usually present in these molecules are responsible for different magnetic behaviors that have encouraged their study as organic- and molecule-based magnets.[6] Furthermore, these systems can be classified as *nondisjoint* or *disjoint* according to the shape of the nonbonding molecular orbitals, which for the latter do not present any atoms in common. Within this category of compounds there is no strong spin-state preference, and the lowest singlet and triplet states appear to be nearly degenerate[7] or, in some cases, to violate Hund's molecular selection rule, according to which the triplet state should be favored, presenting a singlet ground state. The prototype for the disjoint non-Kekulé diradicals is the tetramethylene-ethane[8−12] molecule (TME, Figure 1), for which the experimental characterization of the ground state and of the spin ordering has engaged researchers for many decades. First electron paramagnetic resonance (EPR) experiments at various conditions done by P. Dowd[8,9] reported intense triplet signals which persisted indefinitely at low temperatures. These results, that seemed to confirm the triplet state to be the correct ground state, were later contradicted by ion photoelectron spectroscopy (IPS) experiments.[12] The negative ion photo-electron spectra showed that TME is characterized by two low-lying nearly degenerate electronic states. The ground state was assigned to the singlet state ^1A, while the first excited state was found to be the ^3B_u triplet state. The energy difference between

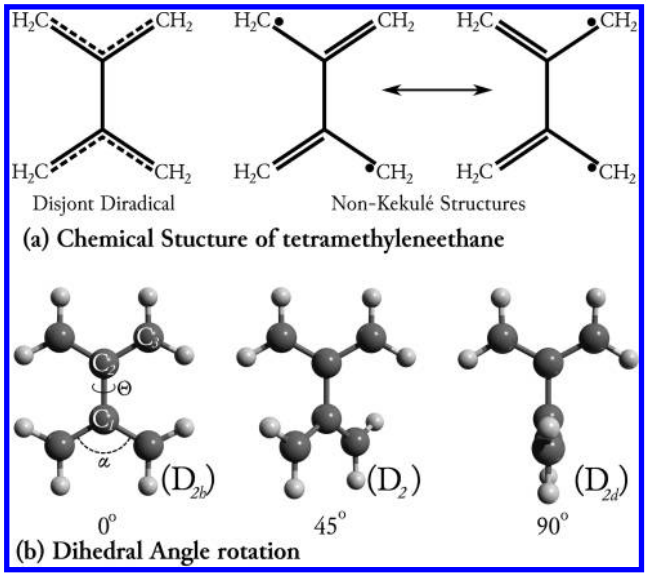

Figure 1. (a) Sketch representation of the electronic structure of TME; the dashed lines represent the delocalization of the π electrons. This state can be described as the superposition of the two non-Kekulé structures shown on the right. (b) Torsion of the central carbon−carbon bond of TME.

Received: August 26, 2015
Published: October 23, 2015

DOI: 10.1021/acs.jctc.5b00819
J. Chem. Theory Comput. 2015, 11, 5696−5704

the two states at 90° was estimated to be equal to 0.130(13) eV. The difference between the IPS and EPR experimental findings was explained in terms of the possible geometrical interconversion of these two nearly degenerate states, that in the EPR experiments could be induced by the interaction with the environment and by temperature effects.

The IPS experiments also characterized the low-lying $^2B_1$ and ^2A states of the anion TME^-[12] whose relative stability was seen to depend on the dihedral angle. For an angle of 90° the $^2B_1$ doublet was found to be more stable than the ^2A one and to lie 0.99(1) eV lower than the ^3B_u triplet state of the neutral TME.

In order to investigate the possible role played by the conformational changes in the interconversion between the two states and to better interpret the experimental findings, the potential energy curves of the low-lying singlet and triplet states of TME have been studied by using different levels of theory, as a function of the torsion of the dihedral angle involving the central carbon−carbon C_1-C_2 bond (Figure 1(b)).[13−22]

Due to the complexity of its electronic ground state, TME represents a challenging system for the methods applied in quantum chemistry, that display a variety of different and often contradicting results. The diradical ^1A singlet state requires at least two configurations to recover the correct *static electronic correlation*, and at the same time the delicate balance between the exchange interaction and the Coulomb repulsion, responsible for the near degeneracy of the low-lying singlet and triplet states, requires an adequate representation of the *dynamical electronic correlation*.[22] For this reason the various results are not at all consistent for the relative stability of the two states with respect to the dihedral angle[17,19,20,22] and for the possible degeneracy[15,18,21] or even relative inversion[17,18] of the two states for a dihedral angle of nearly 45°.

The energetic stability of the singlet with respect to the triplet state for each value of the dihedral angle, first theorized through the molecular orbital theory in ref 13, was confirmed computationally by configuration interaction (CI) calculations including single and double excitations (CISD).[14] In contrast with these first results, later CI calculations, which included virtual orbitals to partially take into account *dynamical electronic correlation*, gave an ^1A state more stable than the ^3B_u only for the D_{2h} and D_{2d} molecular geometries (Figure 1), while the relative stability appeared to be inverted at 45°.[15] This change of stability was also predicted by improved virtual orbital (IVO) complete active space configuration interaction (IVO-CASCI),[21] difference dedicated configuration interaction (DDCI),[17] and spin-restricted ensemble-referenced Kohn−Sham (REKS) calculations.[18]

CASSCF calculations[15,16,22] showed a large dependency on the active space and on the basis set used, and only the inclusion of all six π electrons and π orbitals ((6,6) active space) with at least a cc-pVTZ basis set gave an ordering of the two states in accordance with the IPS experiments for all values of the dihedral angle.[15−17,22] This relative stability was also confirmed through CASPT2 calculations within a basis set convergence study[22] although the form of the potential energy curves appeared to be quite different with respect to those obtained by CASSCF. Multireference coupled cluster (MRCC)[19,20] results greatly depended on the inclusion of the triplet perturbative excitations, otherwise favoring the triplet state with respect to the singlet one. Moreover the MRCCSD-(T) calculations still reported nearly flat potential energy curves for the singlet state and a large gap with respect to the triplet one, excluding possible interconversions due to degeneracy between singlet and triplet states.

Finally, a recent work presented quantum Monte Carlo (QMC)[23,24] calculations on CASSCF(6,6)/cc-pVTZ geometries studying the energy curves of the triplet and singlet states at 0°, 90° and between 40 and 50°.[22] At the variational Monte Carlo (VMC) level the authors reported a possible degeneracy of the potential energy curves, that vanished at the diffusion Monte Carlo (DMC) level, leaving a small gap between the two states with the singlet ^1A state lower in energy.

The VMC calculations were based on the estimation of the energy functional on a previously optimized trial wave function, built from a truncated CASSCF expansion with a Jastrow factor.[22] The DMC approach within the fixed-node approximation,[25] which selects the ground state component from a "mixed" distribution involving the trial wave function with the only constraint given by its nodal surface (hypersurface containing the zeros of the trial wave function),[23,24] was used to give a better estimation of the energy differences between the two states of TME, in the crucial points with dihedral angles of 0°, 90° and between 40 and 50°.[22]

In the present work we further extend the QMC analysis, applying in particular the VMC method with the full optimization of the structural and wave function parameters[26−29] and the lattice regularized diffusion Monte Carlo (LRDMC) method,[30] to give an overall and complete *ab initio* picture of the potential energy curves of the two low-lying electronic states of TME and of its anion TME^-.

Extending the QMC investigation also to the two anionic states of TME^- (^2A and $^2B_1$), whose potential energy curves intersect for a dihedral angle of nearly 40°,[31] enables us to report a more complete comparison with the IPS experimental findings.[12]

Another important goal of this investigation is to study the behavior of the Jastrow Antisymmetrized Geminal Power (JAGP)[32,33] wave function, which is based on the resonating valence bond representation introduced by Pauling for the description of the chemical bonds.[34] The JAGP has been already used in the past to study diradical systems.[35,36] We can enlighten the role played by the different components of the wave function in order to recover the *electronic correlation* by comparing the performance of the JAGP ansatz with a reduced subset, obtained by truncating the geminal expansion in terms of one-electron molecular orbitals (see the next section for details).

The article is organized as follows: in the *Computational Methods* section we review the main features of the JAGP ansatz, showing its reliability for the investigation of diradical species, already tackled in previous works,[35,36] and describe the computational details of the calculations; after presenting our results in the *Results and Discussion* section, we summarize the present findings in the *Conclusions* and comment on the possibility to extend our computational protocol to larger diradical systems.

COMPUTATIONAL METHODS

Jastrow Antisymmetrized Geminal Power. The JAGP ansatz is built as the product of an Antisymmetrized Geminal Power (AGP), a fermionic term describing the nodal surface, and a Jastrow factor,[29,37] a bosonic function including many-particle terms necessary for the correct description of the electron−electron and electron−nucleus cusp conditions[38] and for the recovery of the *dynamical electronic correlation*. For

DOI: 10.1021/acs.jctc.5b00819
J. Chem. Theory Comput. 2015, 11, 5696−5704

closed shell molecular systems of M atoms and N_e electrons in a spin singlet state, i.e. $N_e/2 = N_e^{\uparrow} = N_e^{\downarrow}$, the determinantal AGP part is written as the antisymmetrized product

$$\Psi_{\mathrm{AGP}}(\overline{\mathbf{x}}) = \hat{A} \prod_{i=1}^{N_e/2} \Phi_G(\mathbf{x}_i^{\uparrow}; \mathbf{x}_i^{\downarrow}) \tag{1}$$

of geminal functions of two electrons i and j with opposite spin in a spin singlet state $|0, 0\rangle$

$$\Phi_G(\mathbf{x}_i; \mathbf{x}_j) = \sum_{a,b=1}^{M} \sum_{\mu,\nu} g_{\mu_a\nu_b} \psi_{\mu_a}(\mathbf{r}_i)\psi_{\nu_b}(\mathbf{r}_j)|0, 0\rangle \tag{2}$$

defined as the linear combination of products of two atomic orbitals ψ_{μ_a} and ψ_{ν_b} centered on the a-th and b-th nuclei. The $g_{\mu_a\nu_b}$ coefficients are weights describing the coupling between the two atomic orbitals. $\hat{A}$ is the antisymmetrization operator.

Given a set of orthogonalized molecular orbitals $\varphi_k(\mathbf{r}) = \sum_{a=1}^{M}\sum_{\mu} p_{\mu_a}^k \psi_{\mu_a}(\mathbf{r})$, built as a linear combination of atomic orbitals, the matrix of the geminal coefficients $g_{\mu_a\nu_b}$ can be diagonalized,[37] giving the geminal expansion

$$\Phi_G^{mol}(\mathbf{x}_i; \mathbf{x}_j) = \sum_{k=1}^{n} \lambda_k \varphi_k(\mathbf{r}_i)\varphi_k(\mathbf{r}_j)|0, 0\rangle \tag{3}$$

which is the sum over n doubly occupied molecular orbitals. The projection from eq 2 to eq 3 becomes an exact mapping ($\Phi_G^{mol} = \Phi_G$) when n is equal to the number L of atomic orbitals in the basis set ($n = L$). If $n < L$ the projection is equal to a truncated JAGP defined as JAGPn.[35,37] Explicitly, the AGP multideterminantal expansion is given by inserting the diagonalized geminal expansion defined by eq 3 in eq 1

$$\Psi_{\mathrm{AGP}} = c_0|\Psi_0\rangle + \sum_{k=1}^{N_e/2} \sum_{q=N_e/2+1}^{n} c_{kk}^{qq}|\Psi_{kk}^{qq}\rangle + \sum_{\substack{k,l=1 \\ k\neq l}}^{N_e/2} \sum_{\substack{q,r=N_e/2+1 \\ q\neq r}}^{n} c_{kkll}^{qqrr}|\Psi_{kkll}^{qqrr}\rangle + \ldots \tag{4}$$

where the coefficients are given by

$$c_0 = \prod_{k=1}^{N_e/2} \lambda_k; \qquad c_{kk}^{qq} = c_0\frac{\lambda_q}{\lambda_k}; \qquad c_{kkll}^{qqrr} = c_0\frac{\lambda_q\lambda_r}{\lambda_k\lambda_l}; \qquad \ldots$$

The first term in this expansion represents the leading closed-shell Slater determinant $|\Psi_0\rangle$, whose weight is the product of the λ_k coefficients associated with the doubly occupied $N_e/2$ molecular orbitals in the expansion of eq 3. The $|\Psi_{kk}^{qq}\rangle$ determinants are obtained by the promotion of an electron pair from the molecular orbital $\varphi_k(\mathbf{r}_i)$ ($k \leq N_e/2$) to the unoccupied orbital $\varphi_q(\mathbf{r}_i)$ ($N_e/2 < q \leq n$). At the same time, the determinants $|\Psi_{kkll}^{qqrr}\rangle$ describe two electron pairs excited from two different occupied orbitals to the unoccupied ones $\varphi_q(\mathbf{r}_i)$ and $\varphi_r(\mathbf{r}_i)$ with $N_e/2 < q, r \leq n$. If $n = L$ the mapping is exact, otherwise Ψ_{AGP} reduces to the truncated $\Psi_{\mathrm{AGP}n}$.

In this scheme the Ψ_{AGP} can be seen as a combination of a subset of even electronic excitations. The AGP ansatz for singlet states corresponds to the subsector of the Hilbert space with seniority number Ω equal to zero.[39] The seniority number indicates the number of unpaired electrons in a given configuration. Since in the expansion of eq 4 only doubly occupied molecular orbitals are present, the AGP is formally a $\Omega = 0$ ansatz.

The selection of configurations by the seniority number, instead of by number of excitations for the configuration-interaction expansion of the many-electron wave function, is seen to be more efficient when the static correlation plays a fundamental role (e.g., linear chains of hydrogen atoms[39]). A $\Omega = 0$ ansatz is able to recover the most part of the static correlation. In the case of the AGP, the fact that the molecular orbitals are generated by the diagonalization of the coupling matrix in the geminal representation (i.e., in a correlated reference) makes us confident that the performance of the AGP is beyond $\Omega = 0$ for the treatment of the static correlation. This reduced set of coupled excitations is actually the rotation in the Hilbert space of a set of determinants composed of correlated molecular orbitals, in which all the excitations (including the odd ones) are taken into account,[36,40] but constrained to the even excitations through the λ_k parameters.

In order to describe spin-polarized systems, it is necessary to introduce the so-called generalized Antisymmetrized Geminal Power (GAGP) wave function defined by Coleman.[41,42] Assuming that the number of spin-up electrons exceeds the number of electrons with opposite spin $N_e^{\uparrow} > N_e^{\downarrow}$, the GAGP is built as the antisymmetrized product

$$\Psi_{\mathrm{GAGP}}(\overline{\mathbf{x}}) = \hat{A}\left[\prod_{i=1}^{N_e^{\downarrow}} \Phi_G(\mathbf{x}_i^{\uparrow}; \mathbf{x}_i^{\downarrow}) \prod_{s=1}^{S} \Phi_s(\mathbf{x}_{N^{\downarrow}+s}^{\uparrow})\right] \tag{5}$$

that, along with $N_e^{\downarrow}$ geminal functions (eq 2), contains $S = (N_e^{\uparrow} - N_e^{\downarrow})$ single electron wave functions

$$\Phi_s(\mathbf{x}_i) = \sum_{a=1}^{M} \sum_{\mu} g_{\mu_a}^s \psi_{\mu_a}(\mathbf{r}_i)|\uparrow\rangle \qquad s = 1, \ldots, S \tag{6}$$

that are essentially independent "molecular orbitals" built as the linear combination of atomic orbitals. This ansatz allows us to treat high-spin and radical states using the same computational protocol applied to the closed-shell singlet states.

Computational Details. The QMC calculations have been carried out using the TurboRVB[43] package by S. Sorella and co-workers. In particular, we have applied the linear method[26] with the inclusion of a partial Hessian to accelerate convergence[27] for the optimization of all the parameters of the wave function (including the coefficients and the exponents of the Gaussian basis sets).

The structural optimizations in the VMC framework are based on the adjoint algorithmic differentiation for evaluating the ionic forces described in ref 28 and first used to optimize the structures of the singlet and triplet states of the ethylene molecule.[29] The various TME and TME^{-} structures have been optimized following the procedure used in ref 44 for which the dihedral angle is kept fixed through classical harmonic constraints, while all the other structural parameters are relaxed together with all the parameters of the wave function: this guarantees the correct convergence toward the variational minima in the parametric space.

To verify the convergence of the QMC calculations we have tested two Gaussian basis sets. The core electrons of the carbon atoms are described with the norm-conserving pseudopotentials[45] that include relativistic corrections. Both basis sets used for the AGP part are contracted Gaussian orbitals. For the hydrogen atoms we have used the basis set of (4s3p)/[2s1p] contracted Gaussian orbitals, while the carbon atoms are

DOI: 10.1021/acs.jctc.5b00819
J. Chem. Theory Comput. 2015, 11, 5696−5704

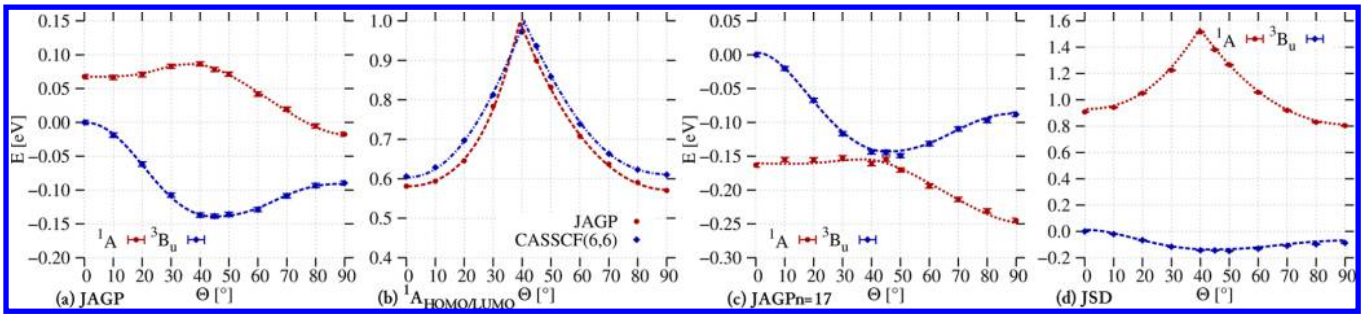

Figure 2. (a), (c), and (d) panels display the VMC energies of the ^1A and ^3B_u states of the neutral TME, calculated on the CASSCF(6,6) geometries reported in ref 22 and rescaled with respect to the energy of the ^3B_u state for a dihedral angle of 0°. In particular the (a) panel displays the energies obtained with the JAGP ansatz, the (c) panel displays the energies obtained by projecting the JAGP on the JAGPn = 17 subspace that includes the LUMO orbital, and the (d) panel displays the energies obtained by projecting the JAGP on a single determinant wave function (JSD). (b) For the ^1A singlet state, comparison between the ratio of the weights of the CASSCF(6,6)/cc-pVTZ configurations with doubly occupied LUMO and HOMO orbitals and the ratio of the λ_{LUMO} and λ_{HOMO} coefficients of the JAGPn = 17 projected wave function (corresponding to the ratio between c_0 and $c_{HOMO^2}^{LUMO^2}$ in eq 4).

Table 1. VMC Energies of the ^1A and ^3B_u States of TME Calculated on the CASSCF(6,6) Structures from Ref 22 for the Planar Geometry[d]

	basis set 1[a]			basis set 2		
	^1A [E_h]	^3B_u [E_h]	ΔE [eV]	^1A [E_h]	^3B_u [E_h]	ΔE [eV]
VMC						
JAGP	−38.61937(12)	−38.62185(11)	0.067(4)	−38.62401(11)	−38.62648(10)	0.067(4)
JAGP[n = 17/(15 + 2)]	−38.61920(12)	−38.61321(11)	−0.163(4)	−38.62374(11)	−38.61801(11)	−0.156(4)
JSD[n = 16/(15 + 2)][b]	−38.57982(12)	−38.61321(11)	0.908(4)	−38.58425(11)	−38.61801(11)	0.919(4)
JCASSCF(6,6)[22]	−38.61172(89)	−38.60317(88)	−0.233(34)			
LRDMC (a = 0.2)[c]						
JAGP	−38.69095(17)	−38.68819(17)	−0.075(6)	−38.69069(17)	−38.68819(16)	−0.068(6)
JAGP[n = 17/(15 + 2)]	−38.69014(17)	−38.68537(18)	−0.129(7)	−38.69032(17)	−38.68548(17)	−0.132(6)
JSD[n = 16/(15 + 2)]	−38.66299(19)	−38.68537(18)	0.609(7)	−38.66292(18)	−38.68548(17)	0.614(7)

[a]The first basis set (basis set 1) is built with (5s5p2d)/[3s2p1d] contracted orbitals for the carbon atoms and (4s3p)/[2s1p] contracted orbitals for the hydrogen atoms. The second basis set (basis set 2) is built using the same contracted orbitals for the hydrogen atoms and (6s5p3d)/[4s3p2d] contracted orbitals for the carbon atoms. The Jastrow factor is always built from uncontracted Gaussian primitives, that correspond in number with the number of contracted orbitals of the fermionic basis set. [b]The notation for the projected JAGP reads as follows: the number of doubly occupied molecular orbitals for the singlet state on the left (16 or 17) and the number of doubly occupied molecular orbitals plus the number of singly occupied molecular orbitals for the triplet state on the right between parentheses (15 + 2). [c]All the LRDMC calculations have been performed using a value of 0.2 for the step a. [d]$\Delta E = E(^1A) - E(^3B_u)$.

represented by (5s5p2d)/[3s2p1d] contracted Gaussian orbitals for the first basis set and by (6s5p3d)/[4s3p2d] for the second basis set.

The basis sets used to build the Jastrow factors only contain uncontracted Gaussian orbitals. For the hydrogen atoms we have used a (2s1p) basis set, while for the carbon atoms the number of orbitals varies from (3s2p1d) for the smallest basis set to (4s3p2d) for the largest one.

In order to give a better estimation of the energy differences we have used the Lattice Regularized Diffusione Monte Carlo (LRDMC) method,[30] based on the Green's Function Monte Carlo method with a space discretization. All the LRDMC calculations are done using a fixed space discretization of a = 0.2 bohr.

The CASSCF and NEVPT2 calculations have been done using the Orca 3.0.3 package.[46] In order to reproduce the results in ref 22 the CASSCF energies of the TME states are obtained in the (6,6) active space and with the cc-pVTZ basis set on the corresponding structures reported in the SI of ref 22. The two anionic states have been investigated using the same basis set and the (7,6) active space. In order to converge to the expected ^2A and $^2B_1$ states predicted by the experimental measurements[12] the state-average procedure has been used.

RESULTS AND DISCUSSION

The first step in our investigation is the study of the behavior of the JAGP ansatz in describing the triplet ^3B_u and singlet ^1A states of TME and their reciprocal ordering. In Figure 2a we have reported the VMC energy profiles of the two states obtained by optimizing the JAGP wave function on the CASSCF(6,6) structures previously calculated in ref 22.

Taken singularly, the two curves are similar to the most accurate references present in the literature and obtained through CASPT2,[22] but their ordering appears reversed with respect to the IPS data.[12]

To understand the reason for this discrepancy, we must first recall that while the triplet ^3B_u state is a single-reference state, properly described by those methods able to recover the *dynamical correlation*, the ^1A diradical state needs a multi-configurational representation to correctly recover the *static correlation*.

Following the projection procedure of the JAGP on a multideterminantal expansion of molecular orbitals,[35−37,40,47]

DOI: 10.1021/acs.jctc.5b00819
J. Chem. Theory Comput. 2015, 11, 5696−5704

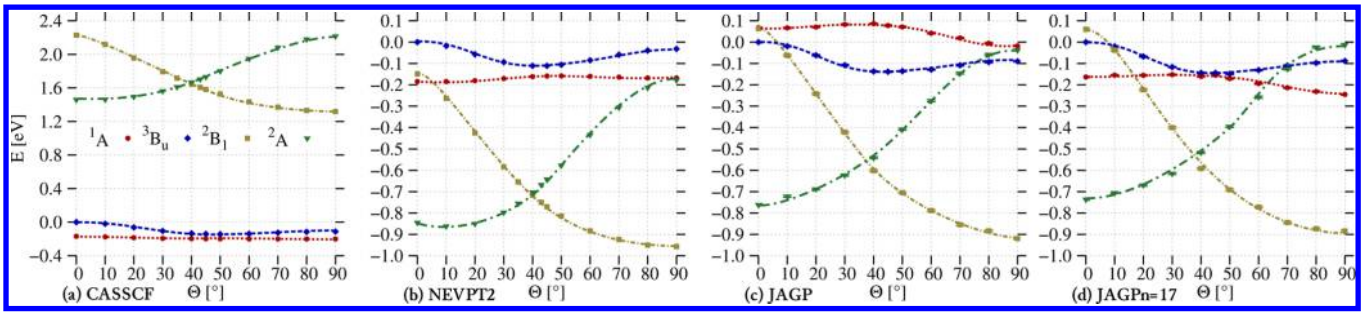

Figure 3. Energies of the singlet ^{1}A and triplet ^{3}B$_u$ states of TME and of the two anionic ^{2}A and ^{2}B$_1$ states of TME$^-$ as a function of the torsion of the dihedral angle. The CASSCF (a), NEVPT2 (b), and VMC (c,d) energy profiles are calculated on the structures obtained from CASSCF(6,6)/cc-pVTZ calculations reported in ref 22 for the two states of TME and from the state average CASSCF(7,6)/cc-pVTZ for the two anionic states of TME$^-$. In panel (c) we report the JAGP results, while in panel (d) those obtained by the JAGPn = 17 wave function include only the LUMO orbital.

i.e. the JAGPn previously described, we can demonstrate that the ansatz is able to well reproduce the degeneracy of the LUMO and HOMO frontier orbitals in diradical species. This can be observed by comparing the ratio of the λ_k coefficients for the HOMO and LUMO molecular orbitals (eq 3)[35] with the weights of the CASSCF(6,6) $(\text{HOMO})^2$ and $(\text{LUMO})^2$ configurations (Figure 2b). In fact, for a dihedral angle of about 40° the ratio becomes equal to one, featuring the exact degeneracy of the two configurations for both AGP and CASSCF(6,6), and thus confirming that both the wave functions are correctly describing the diradical nature of the molecule. Even for the planar geometry the *static electronic correlation* plays a not negligible role, with a ratio around 0.6.

In order to better comprehend the reason for the unexpected energy ordering of the ^{3}B$_u$ and ^{1}A states that could possibly depend on the missing of *static* or *dynamical correlation* or on the unbalanced variational spaces used to describe the two states, various tests have been made.

In Table 1, we have reported different VMC and LRDMC results for these two states on the CASSCF(6,6) geometry at a 0° dihedral angle (D_{2h}) structure by means of the two basis sets described in the previous section and using the JAGP and JAGPn wave functions. Negative values of $\Delta E = E(^1\text{A}) - E(^3\text{B}_u)$ correspond to the singlet lower in energy than the triplet.

The results in Table 1 confirm that the choice of the basis set is less relevant for getting consistent and converged results at both the VMC and LRDMC levels of theory. For this reason we have used the first basis set for all the QMC calculations presented in this work, thus reducing the computational effort. At the LRDMC level the JAGP energies of the ^{3}B$_u$ and ^{1}A states invert their relative stability and appear to be in agreement with the experimental predictions. Still the energy gap between the two states seems greatly underestimated.

By projecting the JAGP on the truncated molecular subspace with $n = 17 = N_e/2 + 1$ (using pseudopotentials for the carbon atoms) orbitals, that includes in the expansion of eq 3 only the LUMO orbital (JAGPn = 17) the energy of the ^{1}A state does not change with respect to the JAGP one, while the energy of the ^{3}B$_u$ triplet state is seen to increase. For the triplet state, the n = 16 and n = 17 molecular orbitals are singly occupied (n = 15 + 2 in Table 1). Using the JAGPn = 17 wave function the energy differences ΔE at the LRDMC and VMC levels substantially coincide (Table 1), and the ordering of the two states corresponds to the one predicted by IPS experiments[12] (Figure 2c and Table S1 of the Supporting Information (SI)). This result gives evidence that the unexpected ordering of the two states for the JAGP ansatz is due to the different variational spaces used to describe the ^{3}B$_u$ and ^{1}A states of TME, that become therefore not directly comparable. In the singlet state the geminal expansion (one geminal function for all electronic pairs) must describe the disjoint diradical character of the state, while for the triplet state it is only used to describe the closed-shell electrons recovering the *dynamical correlation*. The fact that the triplet state only needs *dynamical correlation* is also confirmed at the CASSCF(6,6) level for which at 45° the weight of the second configuration is less than 4% of the total wave function. Thus, in the triplet state the unpaired electrons are described through singly occupied molecular orbitals, and consequently the AGP has, in the triplet case, more variational freedom to describe the *dynamical correlation* through its multideterminantal character. This is why, through the projection on a limited set of molecular orbitals n = 15 + 2, the triplet state loses variational energy, without changing the form of the potential energy curve and giving ^{3}B$_u$ and ^{1}A comparable profiles.

If the LUMO orbital is excluded in the projection of the singlet state (JAGPn = 16) a single-configuration wave function is obtained for which the torsion barrier of the singlet state at 40° diverges (Figure 2d); as already verified for different single-reference methods.[22]

Another interesting effect of this projection can be seen by comparing the potential energy curves of TME and TME$^-$ (^{2}A and ^{2}B$_1$) obtained with the JAGP and JAGPn = 17 wave functions. In order to be consistent with our previous calculations, the potential energy curves of the two anionic states have been calculated on the optimized structures at the CASSCF(7,6)/cc-pVTZ level of theory, obtained using the state average procedure. The CASSCF energies for the four states are reported in Figure 3a. Before commenting further on our QMC results, it is important to underline that, as already stated in previous CASPT2 investigations,[17,18,21,22] the lack of *dynamical correlation* in CASSCF has a huge effect on the shape of the potential energy curves and on the relative stability of the anionic states with respect to those of the neutral molecule: the anionic states at CASSCF lie well above the neutral ones, independently of the value of the dihedral angle, contradicting the experimental IPS findings that reveal the anion to be energetically favored with respect to the neutral TME at 90°.[12] The low-lying anionic state at a dihedral angle of 90° has been experimentally assigned to ^{2}B$_1$, but two anionic states have been theoretically predicted to intersect at a dihedral angle of about 45° and to be separated by conformational differences.[12]

DOI: 10.1021/acs.jctc.5b00819
J. Chem. Theory Comput. 2015, 11, 5696−5704

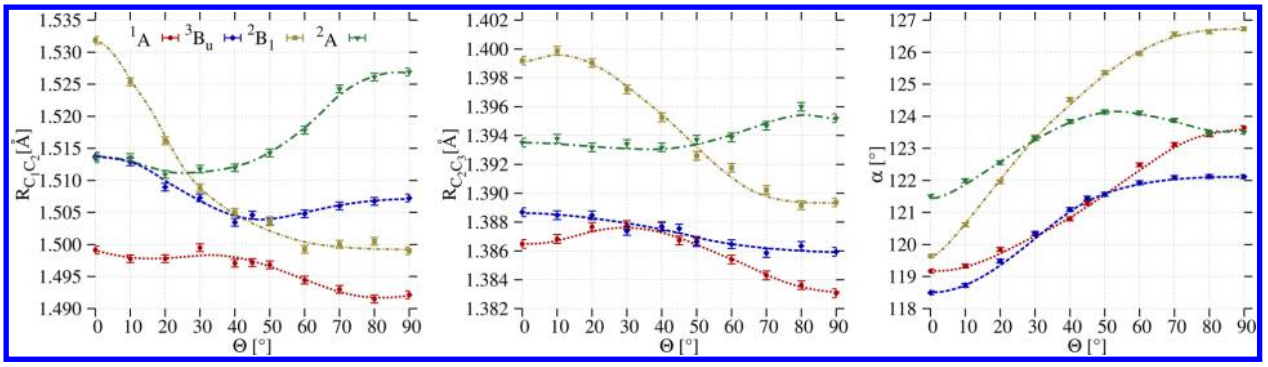

Figure 4. Geometric parameters of the ^{1}A, ^{3}B$_u$, ^{2}A, and ^{2}B$_1$ states of TME (C_1C_2 and C_2C_3 bonds and the α molecular angle) as functions of the torsion of the central dihedral angle, obtained with the JAGP wave function and VMC optimization.

Table 2. VMC Geometric Parameters and Energies of the ^{1}A and ^{3}B$_u$ States Obtained with Different Wave Functions and Compared with the CASSCF(6,6) Results from Ref 22

	^{1}A			^{3}B$_u$			VMC		
	C_1C_2 [Å]	C_2C_3 [Å]	CCC [deg]	C_1C_2 [Å]	C_2C_3 [Å]	CCC [deg]	^{1}A [E_h]	^{3}B$_u$ [E_h]	ΔE [eV]
0°									
JAGP[n = 17/(15 + 2)]	1.4993(4)	1.3867(2)	119.29(2)	1.5121(4)	1.3881(2)	118.29(3)	−38.62060(12)	−38.61530(12)	−0.144(5)
JAGP	1.4992(2)	1.3865(2)	119.17(2)	1.5138(4)	1.3887(2)	118.50(1)	−38.62086(11)	−38.62223(12)	0.037(5)
JCAS[a22]	1.49246	1.39395	118.258	1.50801	1.39327	118.008	−38.61172(89)	−38.60317(88)	−0.233(34)
JAGP[n = 17/(15 + 2)][a]							−38.61920(12)	−38.61321(11)	−0.163(4)
JAGP[a]							−38.61937(12)	−38.62185(11)	0.067(4)
45°									
JAGP[n = 17/(15 + 2)]	1.4992(2)	1.3869(2)	121.33(1)	1.5013(2)	1.3863(1)	121.37(1)	−38.62038(12)	−38.62003(12)	−0.009(5)
JAGP	1.4978(3)	1.3867(2)	121.27(1)	1.5044(4)	1.3865(2)	121.39(2)	−38.61972(12)	−38.62799(11)	0.225(5)
JCAS[a22]	1.49579	1.39175	120.776	1.50237	1.39051	120.914	−38.60868(85)	−38.61070(84)	0.055(32)
JAGP[n = 17/(15 + 2)][a]							−38.61889(11)	−38.61852(12)	−0.010(5)
JAGP[a]							−38.61899(12)	−38.62695(11)	0.217(5)
90°									
JAGP[n = 17/(15 + 2)]	1.4944(4)	1.3827(2)	123.76(2)	1.5066(4)	1.3850(2)	122.15(2)	−38.62444(12)	−38.61780(12)	−0.181(5)
JAGP	1.4922(4)	1.3831(2)	123.65(2)	1.5072(4)	1.3859(2)	122.12(2)	−38.62355(11)	−38.62609(11)	0.069(5)
JCAS[a22]	1.49810	1.38809	122.546	1.50530	1.38949	121.832	−38.61117(86)	−38.60805(87)	−0.085(33)
JAGP[n = 17/(15 + 2)][a]							−38.61920(12)	−38.61321(11)	−0.163(4)
JAGP[a]							−38.62250(11)	−38.62515(11)	0.072(5)

[a]These QMC results are obtained using the molecular structures calculated with the CASSCF(6,6) method from ref 22.

The wrong behavior of CASSCF is corrected by perturbative contributions to the electronic state: in fact in the NEVPT2 calculations reported in Figure 3b the ordering of the two anionic states is consistent with the experimental findings.

Finally, we have reported the VMC results on the CASSCF structures for the ^{2}A and ^{2}B$_1$ states, using the JAGP and JAGPn = 17 wave functions, in Figures 3c and 3d (see also Table S1). Due to the fact that the anionic states are separated by strong conformational differences, it is possible to perform a stable optimization within the same variational space in VMC for both the anionic states.

Even if through the projection all the single-configuration states (^{3}B$_u$, ^{2}B$_1$, and ^{2}A) lose variational energy, their relative energies remain unchanged; as shown in Table 1. Both the full JAGP and the truncated JAGPn = 17 are seen to be accurate for describing the relative stability between the anion and the neutral systems: the two anionic states cross at around 40°, and the ^{2}A is more stable than ^{2}B$_1$ for the planar geometry, while the opposite is found at 90°.

As already reported, the total energy of the ^{1}A singlet state is not substantially affected by the truncation of the AGP, thus modifying all the energy differences with the other states of TME and TME$^-$. The JAGPn = 17 corresponds to a single configuration for the ^{3}B$_u$, ^{2}B$_1$, and ^{2}A states, and the projection of the JAGP removes most of the *dynamical correlation* recovered by the AGP multideterminantal expansion for these three states (obviously the Jastrow term is not affected by the truncation), without changing their relative physical properties.

Once the reliability of the methodological approach is verified (at least using the reduced ansatz), we have performed the structural optimizations through the JAGP/VMC protocol,[29] computing the energy profiles of the four electronic states of TME and TME$^-$ in order to explore the possible correlations between the structural parameters and the energy profiles. In Figure 4 the main molecular parameters are displayed as a

DOI: 10.1021/acs.jctc.5b00819
J. Chem. Theory Comput. 2015, 11, 5696−5704

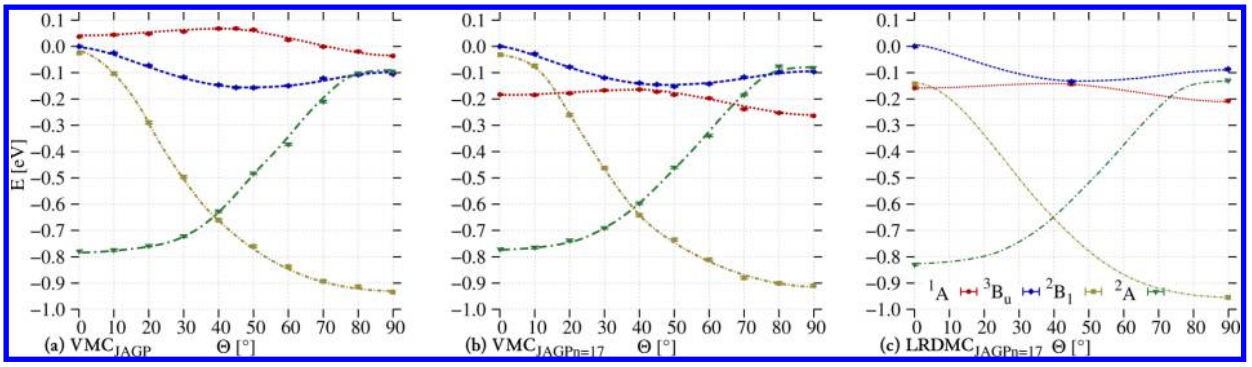

Figure 5. QMC energies of the states of TME and TME$^-$ as a function of the torsion of the dihedral angle, calculated on the JAGP optimized structures: (a) VMC results on the JAGP wave function, (b) VMC results on the projected JAGPn = 17 wave function, and (c) LRDMC results on the projected JAGPn = 17 obtained for a few structures.

function of the dihedral angle (Table S2 of the SI). The central bond C_1C_2 is formally a single bond in all the TME and TME$^-$ states. Changes in the C_1C_2 value along the torsion are quite small (≤10 mÅ) for both the singlet ^{1}A and triplet ^3B_u states and qualitatively seem to follow the corresponding energy profile obtained by the JAGPn = 17 (Figure 2c). Moreover, around 30°−35° both the value of the C_2C_3 bond and of the α angle of the two states become degenerate, and only a small difference in the C_1C_2 bond length remains.

To ascertain possible structural differences between the JAGP and the reduced JAGPn = 17 subspace, we have compared in Table 2 the structures of the two spin states of neutral TME, obtained for 0°, 45°, and 90° dihedral angles.

The predicted structures are identical when looking at the C_2C_3 bonds and at the α angle, but the JAGPn = 17 predicts a constant C_1C_2 elongation for the ^{1}A state and a shortening for the ^3B_u state, both of about 1 mÅ. This means that the gap between the two bonds in Figure 4a, with the JAGPn = 17 subspace, diminishes by 2 mÅ but still does not close, avoiding the structural degeneracy of the ^3B_u and ^{1}A states, as predicted by Restricted Ensemble Kohn−Sham (REKS) DFT calculations.[18]

The added electron in the ^{2}A and $^2B_1$ states of TME$^-$ produces a general larger rearrangement of the geometric parameters along the torsion path (Figure 4). In particular, as the dihedral angle increases from the D_{2h} planar geometry, a larger increase (decrease) of C_1C_2 is seen for the anionic ^{2}A ($^2B_1$) state, similar to the trend of the formally double C_2C_3 bond. The decrease of the bond lengths in the $^2B_1$ state and the opening of the α angle can be interpreted as an increased conjugation along the carbon skeleton that leads to larger electron delocalization along the molecule. On the other hand, we face the opposite situation in the case of the ^{2}A state, for which the single C_1C_2 bond increases (of a larger percentage with respect to the C_2C_3 bond).

On these JAGP structures we have recomputed the VMC energy profiles using JAGP and JAGPn = 17, reported in Figure 5a and Figure 5b, respectively, for the four states of TME and TME$^-$, and assuming the energy of the ^3B_u state at 0° as reference. The LRDMC energies correcting the VMC values for JAGPn = 17 are reported in Figure 5c for the 0°, 45° (only for the neutral TME), and 90° geometries.

The overall picture is very similar to that given by QMC on CASSCF structures and reported in Figures 3c and 3d. Structural effects are however present and not negligible. Looking at the VMC profiles with the JAGPn = 17 ansatz, the JAGP structure is responsible for the inversion in the stability of the $^2B_1$ and ^3B_u states at 0° and for a reduced gap (defined as the absolute value of the energy differences taken into account) between ^3B_u and ^{2}A at 90°.

Two maxima for the ^3B_u state are clearly visible at 0° and 90° with barrier heights with respect to the minimum, respectively, of 0.143(5) eV and 0.046(5) eV at the VMC level (Table S3 of the SI) and of 0.134(7) eV and 0.047(7) eV at the LRDMC level of theory (Table S4 of the SI). For the ^{1}A singlet state we can identify two minima at 0° and 90° being the latter clearly the absolute one. The maximum is predicted to be around 40°−45°, coincident with the value in which the two anionic states intersect. At 0° the barrier is about 0.019(5) eV at the VMC level and of 0.015(7) eV at the LRDMC level of theory, while the barrier for 90° is about 0.091(5) eV at the VMC level and it lowers to 0.064(7) eV at the LRDMC level of theory.

The singlet state is more stable than the triplet one along the path, and while the $^3B_u \leftarrow {}^1$A gap at 0° is equal to 0.183(5) eV at the VMC level, LRDMC predicts a slightly smaller gap of 0.158(7) eV. At 90° the $^3B_u \leftarrow {}^1$A gap is smaller, for VMC it is about 0.168(5) eV, while it is about 0.120(7) eV for LRDMC calculations, in very good agreement with the experimental value of 0.130(13) eV obtained from IPS experiments.[12] As reported by the authors, this vertical gap between the two states overestimates by approximately 0.04 eV the real adiabatic gap between the ^3B_u minimum at 45° and the ^{1}A singlet minimum at nearly 90°: this adiabatic gap is about 0.092(5) eV for VMC and of 0.073(7) eV for LRDMC, compatible with the experimental prevision of 0.087 eV[12] and with previous DMC calculations.[22]

The structure of the neutral TME at 90° is always more stable than the planar one, at variance with the results obtained from the perturbative methods, compatible with the smaller steric effect that reduces the electronic repulsion.

The gap at 45° is close but different from zero, 0.027(4) eV for VMC and of 0.009(7) eV for LRDMC calculations, smaller than that calculated through the perturbative approaches, or by other *ab initio* methods. This reduced gap may also depend on small differences in the elongation of the C_1C_2 bond between the ^3B_u and ^{1}A states, as discussed above, and may close due to the interaction with the gas matrices in EPR experiments,[8,9] thus explaining the persistent triplet signal at low temperature.

The vertical VMC energy gaps between the anionic $^2B_1$ state and the two spin states of TME at 90° are both slightly underestimated with respect to the experimental findings, but this is not due to the projection of the JAGP on the JAGPn =

DOI: 10.1021/acs.jctc.5b00819
J. Chem. Theory Comput. 2015, 11, 5696−5704

17 subspace: indeed the relative energies of the two anionic states, with respect to the ^3B_u state, remain substantially unaffected by the projection, as already pointed out. The IPS[12] $^3B_u \leftarrow {}^2B_1$ gap is reported to be of 0.99(1) eV, while VMC gives a value of 0.814(6) eV. The LRDMC results correct this energy to 0.867(7) eV. At the same time the experimental $^1A \leftarrow {}^2B_1$ gap is equal to 0.86(1) eV,[12] while our VMC and LRDMC calculations predict respectively a gap of about 0.646(7) eV and 0.747(7) eV. VMC and LRDMC energy gaps along the JAGP path are reported in Tables S3 and S4 of the SI. This in part may indicate the necessity to improve the description of the *dynamical correlation* for the anionic states but, on the other hand, also depends on the fact that in QMC the ^3B_u state is nearly 0.1 eV more stable at 90° than at 0°, while this relative stability reduces to less than 0.05 eV for the perturbative approaches,[22] increasing the vertical $^3B_u \leftarrow {}^2B_1$ excitation energy.

A further comparison between our VMC energy profiles and those obtained by NEVPT2 calculations (Figure 3a), although displaying an overall compatibility, reveals two principal differences. First, in VMC the $^3B_u \leftarrow {}^1A$ gap between the two states of TME is smaller with respect to that predicted by NEVPT2 or CASPT2.[22] Second, VMC does not confirm the minimum of the ^2A anionic state at 15°, found in NEVPT2.

CONCLUSIONS

In this work we have studied the potential energy curves of the triplet and singlet states of the neutral TME (^3B_u and ^1A) and of the two low-lying states of the TME^- anion ($^2B_1$ and ^2A) by means of quantum Monte Carlo methods and using the JAGP ansatz.

One aim of this work has been to study the behavior of the JAGP ansatz in describing the simplest prototype of disjoint non-Kekulé diradicals, the TME molecule. In fact, it has already been shown[35,36] that the JAGP ansatz is able to correctly treat the degeneracy between the LUMO and HOMO molecular orbitals, which characterizes pure diradical molecules, and is ascribed to what is defined as *static electronic correlation*.

The application of the full JAGP wave function is characterized by a wrong energy reordering of the triplet and singlet states of TME which contradict the IPS experimental findings.[12] The triplet state has been found to be more stable than the singlet one, even though the two potential energy curves, if singularly studied, correctly describe the expected behavior as a function of the dihedral angle.

To understand the reason for this finding, we have projected the AGP ansatz on the smallest subspace able to properly describe the *static electronic correlation* of the ^1A state, i.e. the JAGPn = 17 space, including only the LUMO as a virtual orbital. The JAGPn = 17 wave function does not change the value of the variational energies and the shape of the curve of ^1A with respect to the torsion of the dihedral angle. This demonstrates that the subspace is still able to correctly reproduce the diradical nature of the singlet state.

The projection on the JAGPn = 17 space for the single-configuration states (^3B_u of the neutral TME and the two $^2B_1$ and ^2A for TME^-) leaves the energy profiles along the torsion coordinate unchanged and also conserves the corresponding energy gaps. However, the absolute energies of these states increase of nearly the same quantity, leading to the expected inversion between the triplet and the singlet energy curves.

This behavior surely needs further investigation, though it is evident that the AGP does not uniformly describe all four electronic states. For the three single-configuration states, for which the unpaired electrons are described by independent molecular orbitals, the closed-shell part of the AGP can use its intrinsic resonating valence bond nature to couple all the closed-shell electronic pairs, recovering the *dynamical correlation* between them. For the singlet state, the geminal function must also describe the diradical nature of the pair of two electrons, that are delocalized on the different carbon atoms and are responsible for the diradical character. This electronic state would require a larger variational space to be described consistently with the three single-configuration states. In other words, the AGP may be missing the spin polarization contribution[48] that stabilizes the singlet state more than the triplet and is responsible for the violation of Hund's rule. Only one geminal could not be enough to describe at the same level of accuracy the different electron pairs in the singlet state of TME.

The present VMC results, with the JAGPn = 17 and JAGP, display however an absolute energy which is always lower than the one obtained from previous VMC calculations (of about 0.01 E_h), obtained using a truncated CASSCF(6,6) wave function multiplied by a Jastrow factor and the same pseudopotential of this work for the carbon atoms.[22]

Once the ansatz has been extensively studied, a full structural optimization of the four states of TME and TME^- has been performed.

The second aim of this work has been in fact to compute the structures of the four states along the torsion path, in order to enlighten possible energetic interconversions triggered by geometric factors. Due to the different symmetry of the two anionic states, we have been able to fully optimize their structures in a stable way through VMC, without the necessity to use a state average procedure.

Within the JAGPn = 17 reduced space, all four *ab initio* torsion barriers are found to be in good agreement with the experimental IPS[12] findings and confirm the possible energetic interconversions supposed to justify the contradictions between IPS and previous EPR experiments.[8,9] The theoretical quantitative prediction of several energy gaps of TME and TME^- shown in this work represents a fundamental step for the application of QMC to more complex molecular systems; however, further investigations must be directed in understanding the behavior of the AGP ansatz in describing chemical systems such as disjoint non-Keluké diradicals, toward which this work represents a pioneering step.

ASSOCIATED CONTENT

Supporting Information

The Supporting Information is available free of charge on the ACS Publications website at DOI: 10.1021/acs.jctc.5b00819.

VMC and LRDMC results with several choices of the subspace of the JAGP for TME and TME^- are collected in tables, together with a comparison among the geometric parameters computed at different levels of theory (PDF)

AUTHOR INFORMATION

Corresponding Authors

*E-mail: matteo.barborini@nano.cnr.it.
*E-mail: coccia@lct.jussieu.fr.

DOI: 10.1021/acs.jctc.5b00819
J. Chem. Theory Comput. 2015, 11, 5696−5704

Notes

The authors declare no competing financial interest.

■ ACKNOWLEDGMENTS

Computational resources have been granted by CINECA through the IscrC_TMERVB project.

■ REFERENCES

(1) Berson, J. A. *Acc. Chem. Res.* **1997**, *30*, 238−244.
(2) Cramer, C. J. *J. Chem. Soc., Perkin Trans. 2* **1998**, 1007−1014.
(3) Lineberger, W. C.; Borden, T. W. *Phys. Chem. Chem. Phys.* **2011**, *13*, 11792−11813.
(4) Salem, L.; Rowland, C. *Angew. Chem., Int. Ed. Engl.* **1972**, *11*, 92−111.
(5) Abe, M. *Chem. Rev.* **2013**, *113*, 7011−7088.
(6) Miller, J. S. *Mater. Today* **2014**, *17*, 224−235.
(7) Davidson, E. R.; Borden, W. T. *J. Am. Chem. Soc.* **1977**, *99*, 2053−2060.
(8) Dowd, P. *J. Am. Chem. Soc.* **1970**, *92*, 1066−1068.
(9) Dowd, P.; Chang, W.; Paik, Y. H. *J. Am. Chem. Soc.* **1986**, *108*, 7416−7417.
(10) Bush, L. C.; Heath, R. B.; Feng, X. W.; Wang, P. A.; Maksimovic, L.; Song, A. I.; Chung, W.-S.; Berinstain, A. B.; Scaiano, J. C.; Berson, J. A. *J. Am. Chem. Soc.* **1997**, *119*, 1406−1415.
(11) Bush, L. C.; Maksimovic, L.; Feng, X. W.; Lu, H. S. M.; Berson, J. A. *J. Am. Chem. Soc.* **1997**, *119*, 1416−1427.
(12) Clifford, E. P.; Wenthold, P. G.; Lineberger, C. W.; Ellison, G. B.; Wang, C. X.; Grabowski, J. J.; Vila, F.; Jordan, K. D. *J. Chem. Soc., Perkin Trans. 2* **1998**, 1015−1022.
(13) Longuet-Higgins, H. C. *J. Chem. Phys.* **1950**, *18*, 265−274.
(14) Du, P.; Borden, W. T. *J. Am. Chem. Soc.* **1987**, *109*, 930−931.
(15) Nachtigall, P.; Jordan, K. D. *J. Am. Chem. Soc.* **1993**, *115*, 270−271.
(16) Nachtigall, P.; Jordan, K. D. *J. Am. Chem. Soc.* **1992**, *114*, 4743−4747.
(17) Rodríguez, E.; Reguero, M.; Caballol, R. *J. Phys. Chem. A* **2000**, *104*, 6253−6258.
(18) Filatov, M.; Shaik, S. *J. Phys. Chem. A* **1999**, *103*, 8885−8889.
(19) Pittner, J.; Nachtigall, P.; Čársky, P.; Hubač, I. *J. Phys. Chem. A* **2001**, *105*, 1354−1356.
(20) Bhaskaran-Nair, K.; Demel, O.; Šmydke, J.; Pittner, J. *J. Chem. Phys.* **2011**, *134*, 154106.
(21) Chattopadhyay, S.; Chaudhuri, R. K.; Sinha Mahapatra, U. *ChemPhysChem* **2011**, *12*, 2791−2797.
(22) Pozun, Z. D.; Su, X.; Jordan, K. D. *J. Am. Chem. Soc.* **2013**, *135*, 13862−13869.
(23) Foulkes, W. M. C.; Mitas, L.; Needs, R. J.; Rajagopal, G. *Rev. Mod. Phys.* **2001**, *73*, 33−83.
(24) Kolorenč, J.; Mitas, L. *Rep. Prog. Phys.* **2011**, *74*, 026502.
(25) Reynolds, P. J.; Ceperley, D. M.; Alder, B. J.; Lester, W. A. *J. Chem. Phys.* **1982**, *77*, 5593.
(26) Umrigar, C. J.; Toulouse, J.; Filippi, C.; Sorella, S.; Hennig, R. G. *Phys. Rev. Lett.* **2007**, *98*, 110201.
(27) Sorella, S.; Casula, M.; Rocca, D. *J. Chem. Phys.* **2007**, *127*, 014105.
(28) Sorella, S.; Capriotti, S. *J. Chem. Phys.* **2010**, *133*, 234111.
(29) Barborini, M.; Sorella, S.; Guidoni, L. *J. Chem. Theory Comput.* **2012**, *8*, 1260−1269.
(30) (a) Casula, M.; Filippi, C.; Sorella, S. *Phys. Rev. Lett.* **2005**, *95*, 100201;(b) Casula, M.; Moroni, S.; Sorella, S.; Filippi, C. *J. Chem. Phys.* **2010**, *132*, 154113.
(31) Müller, B.; Bally, T.; Gerson, F.; de Meijere, A.; von Seebach, M. *J. Am. Chem. Soc.* **2003**, *125*, 13776−13783.
(32) Casula, M.; Sorella, S. *J. Chem. Phys.* **2003**, *119*, 6500.
(33) Casula, M.; Attaccalite, C.; Sorella, S. *J. Chem. Phys.* **2004**, *121*, 7110.
(34) Pauling, L. *The Nature of the Chemical Bond*, 3rd ed.; Cornell University Press; Ithaca, NY, 1960; pp 230−240.
(35) Zen, A.; Coccia, E.; Luo, Y.; Sorella, S.; Guidoni, L. *J. Chem. Theory Comput.* **2014**, *10*, 1048−1061.
(36) Zen, A.; Coccia, E.; Gozem, S.; Olivucci, M.; Guidoni, L. *J. Chem. Theory Comput.* **2015**, *11*, 992−1005.
(37) Marchi, M.; Azadi, S.; Casula, C.; Sorella, S. *J. Chem. Phys.* **2009**, *131*, 154116.
(38) Drummond, N. D.; Towler, M. D.; Needs, R. J. *Phys. Rev. B: Condens. Matter Mater. Phys.* **2004**, *70*, 235119.
(39) (a) Bytautas, L.; Henderson, T. M.; Jimenez-Hoyos, C. A.; Ellis, J. K.; Scuseria, G. E. *J. Chem. Phys.* **2011**, *135*, 044119;(b) Bytautas, L.; Scuseria, G. E.; Ruedenberg, K. *J. Chem. Phys.* **2015**, *143*, 094105.
(40) Barborini, M.; Guidoni, L. *J. Chem. Theory Comput.* **2015**, *11*, 508−517.
(41) Coleman, A. J. *Rev. Mod. Phys.* **1963**, *35*, 668−687.
(42) Coleman, A. J. *J. Math. Phys.* **1965**, *6*, 1425−1431.
(43) Sorella, S. TurboRVB Quantum Monte Carlo package. http://people.sissa.it/sorella/web/index.html (accessed September 30, 2015).
(44) Barborini, M.; Guidoni, L. *J. Chem. Phys.* **2012**, *137*, 224309.
(45) (a) Trail, J. R.; Needs, R. J. *J. Chem. Phys.* **2005**, *122*, 174109;(b) Trail, J. R.; Needs, R. J. *J. Chem. Phys.* **2005**, *122*, 014112.
(46) Neese, F. *WIREs Comput. Mol. Sci.* **2012**, *2*, 73−78.
(47) Barborini, M.; Guidoni, L. *J. Chem. Theory Comput.* **2015**, *11*, 4109−4118.
(48) (a) Kollmar, H.; Staemmler, V. *Theor. Chim. Acta* **1978**, *48*, 223−239;(b) Hrovat, D. A.; Borden, W. T. *J. Mol. Struct.: THEOCHEM* **1997**, *398*−*399*, 211−220.

DOI: 10.1021/acs.jctc.5b00819
J. Chem. Theory Comput. 2015, 11, 5696−5704